Journal of Molecular Liquids 212 (2015) 576–584

Contents lists available at ScienceDirect

Journal of Molecular Liquids

journal homepage: www.elsevier.com/locate/molliq

Geometrical structure, molecular docking and potentiometric studies of Schiff base ligand

A.A. El-Bindary *, A.F. Shoair, A.Z. El-Sonbati, M.A. Diab, E.E. Abdo

Chemistry Department, Faculty of Science, Damietta University, Damietta 34517, Egypt

ARTICLE INFO

Article history:
Received 13 July 2015
Received in revised form 28 September 2015
Accepted 5 October 2015
Available online xxxx

Keywords:
Schiff base
Molecular structure
Molecular docking
Potentiometry

ABSTRACT

Schiff base ligand of 4-(((2-hydroxynaphthalen-1-yl)methylene)amino)-1,5-dimethyl-2-phenyl-1,2-dihydro-3*H*-pyrazol-3-one (**HL**) was synthesized and characterized by IR spectroscopy. The molecular structure of the ligand is optimized theoretically and the quantum chemical parameters are calculated. Molecular docking was used to predict the binding of the ligand with the receptor of prostate cancer 2q7k-hormone and 3hb5-oxidoreductase receptor of breast cancer. The proton–ligand dissociation constant of **HL** and its metal stability constants with Mn^{2+}, Co^{2+}, Ni^{2+} and Cu^{2+} have been determined potentiometrically. The potentiometric studies were carried out in 0.1 M KCl and 20% (by volume) DMF–water mixture. At constant temperature the stability constants of the formed complexes increase in the order of $Cu^{2+} > Ni^{2+} > Co^{2+} > Mn^{2+}$. The effect of temperature was studied at 298, 308 and 318 K and the corresponding thermodynamic parameters (ΔG, ΔH and ΔS) were derived and discussed. The dissociation process is non-spontaneous, endothermic and entropically unfavorable. The formation of the metal complexes has been found to be spontaneous, endothermic and entropically favorable.

© 2015 Elsevier B.V. All rights reserved.

1. Introduction

Schiff bases form an interesting class of chelating ligands that has enjoyed popular use in the coordination chemistry of transition and inner transition metals which show various industrial, biological and catalytic applications. Various studies have shown that, the azomethine group (>C═N–) in Schiff base metal complexes has considerable biological significance and found to be responsible for biological activity such as fungicidal and insecticidal [1]. Structural analyses reveal that hydrazone Schiff base ligands have strong coordination ability, a possibility of keto enol tautomerism and multi-coordination modes [2]. The hydrazones and their metal complexes have many important applications in analytical chemistry and pharmacology [3]. The excited state intramolecular proton transfer (ESIPT) reactions have attracted considerable attention due to their wide range of applications in technology. These reactions are used in the development of laser dyes, optical memories and switches, in the control and measurement of radiation intensity. In this respect, the photochromic compounds have been investigated for many years [4].

The ortho hydroxylated Schiff bases have interesting properties such as photochromism and thermochromism in the solid state and in solution [5,6]. Such compounds can show reversible color changes photo-induced (photochromism) or thermo-induced (thermochromism). Both properties are directly related to the occurrence of intramolecular proton transfer between the hydroxyl oxygen and the imine nitrogen. It is well known that the proton transfer can occur in ground and/or excited state [7–9]. Therefore tautomerization equilibrium exists between enol-imine form (N…H–O) and keto-amine form (N–H…O) occurring through intramolecular proton transfer for 2-hydroxy Schiff base ligands [10,11]. This proton transfer causes a change in the p-electron configuration. However the Schiff bases prepared from 2-hydroxy-1-naphthaldehyde form both type of hydrogen bonds [12,13]. Many Schiff bases derived from 2-hydroxynaphthaldehyde have been studied by NMR spectroscopy and X-ray analysis in the solid state [14–17]. The UV–vis spectra of some 2-hydroxyl Schiff bases have been investigated in polar and non-polar solvent [18–20]. The absorption band at >400 nm belongs to keto-amine form of the Schiff base. The results showed that the enol-imine form is dominant in non-polar solvent while the keto-amine form is dominant in polar solvent for such Schiff bases. Recently, the UV–vis spectroscopic study for quantitative analysis of undefined mixtures of the substituted Schiff bases of 2-hydroxynaphthaldehydes is based on the chemometric approach [19]. Schiff bases can be incorporated into crown ether structures to form interesting cation binding ligands. In such structures the cation can occupy the crown cavity depending on the donor atom and cation character or form the Schiff base complex through the imine group. Some crown ether-containing ortho hydroxylated Schiff bases have been synthesized and their complexation properties with transition metal cations have been investigated [21]. However, the crown ether moieties carrying only oxygen and nitrogen donor atoms exist in these compounds.

* Corresponding author.
E-mail address: abindary@yahoo.com (A.A. El-Bindary).

http://dx.doi.org/10.1016/j.molliq.2015.10.011
0167-7322/© 2015 Elsevier B.V. All rights reserved.

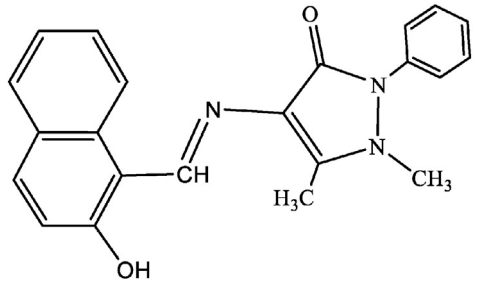

Fig. 1. Structure of Schiff base ligand (**HL**).

In continuation of our previous work [22–24], the present work is centered on the synthesis and characterization of Schiff base derived from the condensation of 2-hydroxy-1-naphthaldehyde with 4-aminoantipyrine. The geometrical structure of Schiff base ligand (**HL**) by HF method with 3-21G basis set was studied. Molecular docking was used to predict the binding of the ligand with the receptor of prostate cancer 2q7k-hormone and 3hb5-oxidoreductase receptor of breast cancer. Furthermore, we report herein the dissociation constant of the Schiff base ligand (**HL**) and the stability constants of its complexes with Mn^{2+}, Co^{2+}, Ni^{2+} and Cu^{2+} at different temperatures. Furthermore, the corresponding thermodynamic functions are evaluated and discussed.

2. Materials and methods

2.1. Preparation of the ligand

Schiff base ligand 4-(((2-hydroxynaphthalen-1-yl)methylene) amino)-1,5-dimethyl-2-phenyl-1,2-dihydro-3*H*-pyrazol-3-one (**HL**) (Fig. 1) was prepared according to the previous procedure [25]. An ethanolic solution of 4-aminoantipyrine (0.1 mmol) was added slowly to the solution of 2-hydeoxy-1-naphthaldehyde (0.1 mmol) in ethanol with constant stirring. The mixture was refluxed for 4 h in a water bath. After concentration of the solution, the precipitate was separated, filtered, washed with ethanol and dried in vacuum desiccator over anhydrous $CaCl_2$.

2.2. Measurements

All the compounds and solvents used were purchased from Aldrich and Sigma and used as received without further purification. The IR spectra were recorded as KBr disks using a Perkin-Elmer 1340 spectrophotometer.

The calculations of geometry optimization were performed using Perkin Elmer ChemBio 3D software by HF method with 3-21G basis set [26,27]. Geometry optimization option was employed to obtain the most stable structure.

In the study simulates the actual docking process in which the ligand–protein pair-wise interaction energies are calculated using Docking Server [28]. The MMFF94 force field was for used energy minimization of ligand molecule using Docking Server. Gasteiger partial charges were added to the ligand atoms. Non-polar hydrogen atoms were merged, and rotatable bonds were defined. Docking calculations were carried out on 2q7k-hormone and 3hb5-oxidoreductase protein model. Essential hydrogen atoms, Kollman united atom type charges, and solvation parameters were added with the aid of AutoDock tools [29]. Affinity (grid) maps of 20 × 20 × 20 Å grid points and 0.375 Å spacing were generated using the Autogrid program [30]. AutoDock parameter set- and distance-dependent dielectric functions were used in the calculation of the Van der Waals and the electrostatic terms, respectively.

The pH measurements were carried out using VWR Scientific Instruments Model 8000 pH-meter accurate to ±0.01 units. The pH-meter readings in the non-aqueous medium were corrected [31]. The electrode system was calibrated according to the method of Irving et al. [32]. Titrations were performed in a double walled glass cell at ionic strength of 0.1 M KCl. Potentiometric measurements were carried out at different temperature. The temperature was controlled to within ±0.05 K by circulating thermostated water (Neslab 2 RTE 220) through the outer jacket of the vessel.

2.3. Potentiometric studies

A ligand solution (0.001 M) was prepared by dissolving an accurately weighted amount of the solid in DMF. Metal ion solutions (0.0001 M) were prepared from metal chlorides in bidistilled water

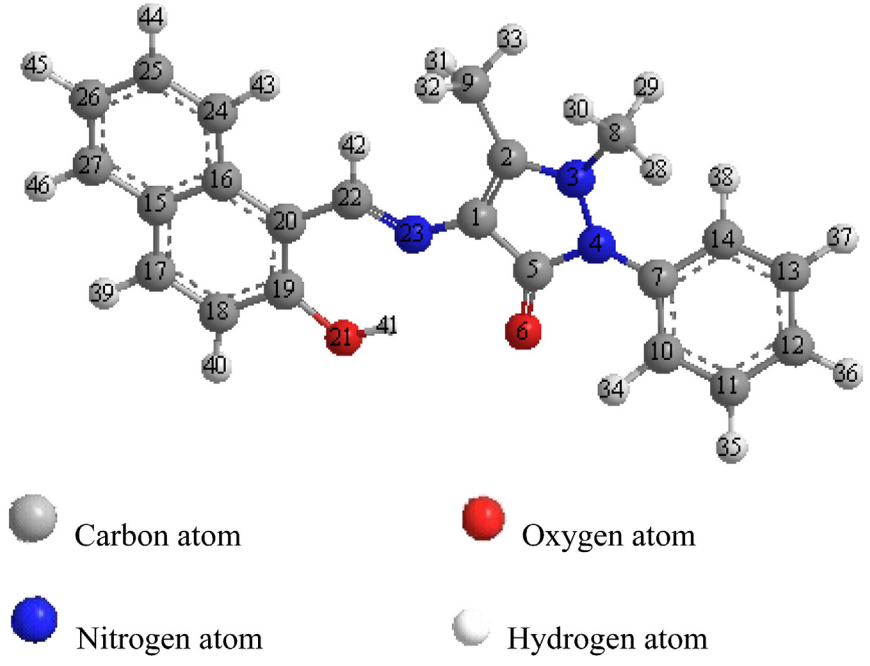

Fig. 2. Molecular structure with atomic numbering for Schiff base ligand (**HL**).

and standardized with EDTA [33]. Solutions of 0.001 M HCl and 1 M KCl were also prepared in bidistilled water. A carbonate-free NaOH solution in 20% (by volume) DMF–water mixture was used as titrant and standardized against oxalic acid.

The apparatus, general conditions and methods of calculation were the same as in previous work [22–24]. The following mixtures (i)–(iii) were prepared and titrated potentiometrically at 298 K against standard 0.02 M NaOH in a 20% (by volume) DMF–water mixture:

i) 5 cm^3 0.001 M HCl + 5 cm^3 1 M KCl + 10 cm^3 DMF.
ii) 5 cm^3 0.001 M HCl + 5 cm^3 1 M KCl + 5 cm^3 DMF + 5 cm^3 0.00 l M ligand.
iii) 5 cm^3 0.001 M HCl + 5 cm^3 l M KCl + 5 cm^3 DMF + 5 cm^3 0.001 M ligand + 10 cm^3 0.0001 M metal chloride.

For each mixture, the volume was made up to 50 cm^3 with bidistilled water before the titration. These titrations were repeated for the temperatures of 308 and 318 K. All titrations have been carried out between pH 4–10 and under nitrogen atmosphere.

3. Results and discussion

3.1. Characterization of the Schiff base ligand (*HL*)

The IR spectrum of the Schiff base ligand (**HL**) is characterized by a very strong carbonyl stretching peak at 1648 cm^{-1} of pyrazole ring [34]. A sharp peak appearing around 1594 cm^{-1} is assigned to ν(C═N) azomethine group, which is characteristic of Schiff bases [35–38]. The region between 1500–900 cm^{-1} is due C–N stretching out-of-plane C–H bending vibrations. The IR spectrum of the ligand show a weak broad band at 3440 cm^{-1} which are assigned to enolic –OH group. The weakness and broadness of these peaks are mainly due to intra-molecular hydrogen bonding between the enolic –OH group with azomethine nitrogen atom of pyrazolone ring [39].

3.2. Geometrical structure

The optimized structure of Schiff base ligand (**HL**) is given in Fig. 2. The bond lengths and bond angles for ligand (**HL**) are listed in Table 1.

Table 1
The selected geometric parameters for Schiff base ligand (**HL**).

Bond lengths (Å)		Bond angles (°)		Bond angles (°)	
C(27)–H(46)	1.104	H(37)–C(13)–C(14)	120.169	C(20)–C(19)–C(18)	118.769
C(26)–H(45)	1.103	H(37)–C(13)–C(12)	119.783	C(20)–C(19)–O(21)	126.037
C(25)–H(44)	1.104	C(14)–C(13)–C(12)	120.044	C(18)–C(19)–O(21)	115.187
C(24)–H(43)	1.099	H(36)–C(12)–C(13)	120.491	C(15)–C(16)–C(24)	115.132
C(22)–H(42)	1.09	H(36)–C(12)–C(11)	120.518	C(15)–C(16)–C(20)	120.217
O(21)–H(41)	0.967	C(13)–C(12)–C(11)	118.99	C(24)–C(16)–C(20)	124.651
C(18)–H(40)	1.104	H(35)–C(11)–C(12)	119.573	C(16)–C(20)–C(19)	119.346
C(17)–H(39)	1.104	H(35)–C(11)–C(10)	120.111	C(16)–C(20)–C(22)	121.281
C(14)–H(38)	1.103	C(12)–C(11)–C(10)	120.314	C(19)–C(20)–C(22)	119.373
C(13)–H(37)	1.103	H(38)–C(14)–C(7)	120.887	H(42)–C(22)–N(23)	113.455
C(12)–H(36)	1.103	H(38)–C(14)–C(13)	116.816	H(42)–C(22)–C(20)	121.079
C(11)–H(35)	1.103	C(7)–C(14)–C(13)	122.266	N(23)–C(22)–C(20)	125.454
C(10)–H(34)	1.101	H(34)–C(10)–C(11)	116.055	C(1)–N(23)–C(22)	131.352
C(9)–H(33)	1.112	H(34)–C(10)–C(7)	121.952	C(1)–C(5)–N(4)	111.093
C(9)–H(32)	1.113	C(11)–C(10)–C(7)	121.961	C(1)–C(5)–O(6)	123.024
C(9)–H(31)	1.112	H(30)–C(8)–H(29)	109.053	N(4)–C(5)–O(6)	125.744
C(8)–H(30)	1.113	H(30)–C(8)–H(28)	103.771	H(33)–C(9)–H(32)	107.971
C(8)–H(29)	1.114	H(30)–C(8)–N(3)	112.568	H(33)–C(9)–H(31)	103.753
C(8)–H(28)	1.112	H(29)–C(8)–H(28)	109.375	H(33)–C(9)–C(2)	112.395
C(18)–C(17)	1.335	H(29)–C(8)–N(3)	110.706	H(32)–C(9)–H(31)	110.294
C(15)–C(17)	1.341	H(28)–C(8)–N(3)	111.122	H(32)–C(9)–C(2)	110.827
C(16)–C(15)	1.354	C(14)–C(7)–C(10)	116.414	H(31)–C(9)–C(2)	111.344
C(27)–C(15)	1.347	C(14)–C(7)–N(4)	119.602	C(2)–N(3)–N(4)	114.409
C(26)–C(27)	1.338	C(10)–C(7)–N(4)	123.965	C(2)–N(3)–C(8)	115.901
C(25)–C(26)	1.337	C(5)–N(4)–N(3)	102.355	N(4)–N(3)–C(8)	129.133
C(24)–C(25)	1.342	C(5)–N(4)–C(7)	130.25	N(3)–C(2)–C(1)	104.075
C(16)–C(24)	1.353	N(3)–N(4)–C(7)	123.336	N(3)–C(2)–C(9)	128.703
C(20)–C(16)	1.363	H(45)–C(26)–C(27)	120.903	C(1)–C(2)–C(9)	127.049
C(19)–C(20)	1.36	H(45)–C(26)–C(25)	120.707	C(2)–C(1)–C(5)	106.932
C(18)–C(19)	1.343	C(27)–C(26)–C(25)	118.389	C(2)–C(1)–N(23)	135.358
C(7)–C(14)	1.349	H(44)–C(25)–C(26)	119.413	C(5)–C(1)–N(23)	117.706
C(13)–C(14)	1.342	H(44)–C(25)–C(24)	120.476		
C(12)–C(13)	1.34	C(26)–C(25)–C(24)	120.111		
C(11)–C(12)	1.34	H(41)–O(21)–C(19)	116.69		
C(10)–C(11)	1.343	H(40)–C(18)–C(17)	118.513		
C(7)–C(10)	1.349	H(40)–C(18)–C(19)	119.305		
N(3)–C(2)	1.277	C(17)–C(18)–C(19)	122.182		
C(1)–C(2)	1.345	H(46)–C(27)–C(15)	121.386		
C(5)–C(1)	1.364	H(46)–C(27)–C(26)	117.701		
N(4)–C(5)	1.273	C(15)–C(27)–C(26)	120.913		
N(3)–N(4)	1.363	H(39)–C(17)–C(18)	118.565		
C(1)–N(23)	1.263	H(39)–C(17)–C(15)	121.917		
C(22)–N(23)	1.26	C(18)–C(17)–C(15)	119.518		
C(20)–C(22)	1.355	H(43)–C(24)–C(25)	113.024		
C(19)–O(21)	1.369	H(43)–C(24)–C(16)	123.716		
C(2)–C(9)	1.508	C(25)–C(24)–C(16)	123.26		
N(3)–C(8)	1.485	C(17)–C(15)–C(16)	119.967		
N(4)–C(7)	1.279	C(17)–C(15)–C(27)	117.84		
C(5)–O(6)	1.216	C(16)–C(15)–C(27)	122.194		

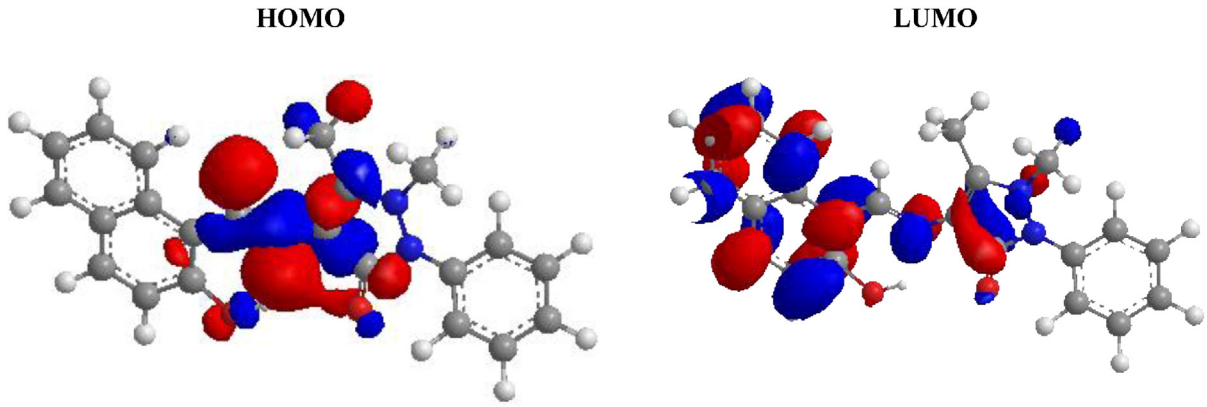

Fig. 3. The Highest Occupied Molecular Orbital (HOMO) and the Lowest Unoccupied Molecular Orbital (LUMO) of Schiff base ligand (**HL**).

The C(22)–N(23) bond with length 1.26 Å for ligand (**HL**) is a normal imine bond.

The HOMO and LUMO are shown in Fig. 3. The HOMO–LUMO energy gap, ΔE, which is an important stability index, is applied to develop theoretical models for explaining the structure and conformation barriers in many molecular systems [40,41]. The value of ΔE for Schiff base ligand (**HL**) was found to be 3.23 eV. The calculated quantum chemical parameters are given in Table 2. Additional parameters such as ΔE, absolute electronegativities, χ, chemical potentials, Pi, absolute hardness, η, absolute softness, σ, global electrophilicity, ω, global softness, S, and additional electronic charge, ΔN_{max}, have been calculated according to the following equations [30,40]:

$$\Delta E = E_{LUMO} - E_{HOMO} \tag{1}$$

$$\chi = \frac{-(E_{HOMO} + E_{LUMO})}{2} \tag{2}$$

$$\eta = \frac{E_{LUMO} - E_{HOMO}}{2} \tag{3}$$

$$\sigma = \frac{1}{\eta} \tag{4}$$

$$Pi = -\chi \tag{5}$$

$$S = \frac{1}{2\eta} \tag{6}$$

$$\omega = \frac{Pi^2}{2\eta} \tag{7}$$

$$\Delta N_{max} = -\frac{Pi}{\eta}. \tag{8}$$

3.3. Molecular docking

Cancer can be described as the uncontrolled growth of abnormal cells. Prostate cancer is the most common non-skin malignancy in men. Except for lung cancer, it is responsible for more deaths than any other cancer. The American Cancer Society (ACS) estimated 1 man in 6 will be diagnosed with prostate cancer during his life time. A little over 1.8 million men in the United States are survivors of prostate cancer [42].

Breast cancer is one of the most recurring worldwide diagnosed and deadliest cancers next to lung cancer with a high number of mortality rates among females [43]. At global level, it accounted for more than 1.6 million new cases in 2010. The incidence or prevalence rate of the breast cancer in India is expected to be more than 90,000 in the coming years and over 50,000 women die each year.

Molecular docking is a key tool in computer drug design [44]. The focus of molecular docking is to simulate the molecular recognition process. Molecular docking aims to achieve an optimized conformation for both the protein and drug with relative orientation between them such that the free energy of the overall system is minimized.

In this context, we used molecular docking between ligand (**HL**) and prostate cancer mutant 2q7k-hormone and breast cancer (3hb5). The results showed a possible arrangement between ligand (**HL**) and receptor (2q7k, 3hb5). The docking study showed a favorable interaction between ligand (**HL**) and the receptor (2q7k, 3hb5) and the calculated energy is listed in Table 3, and Figs. 4(A, B) and 5(A1, B1) for receptor 2q7k and 3hb5, respectively. According to the results obtained in this study, HB plot curve indicates that, the Schiff base ligand (**HL**) binds to the two proteins with hydrogen bond interactions and decomposed interaction energies in kCal/mol exist between the of Schiff base ligand (**HL**) with 2q7k and 3hb5 receptors as shown in Fig. 6. The calculated efficiency is favorable where k_i values estimated by AutoDock were compared with experimental k_i values, when available, and the Gibbs free energy is negative. Also, based on this data, we can propose that interaction between the 2q7k and 3hb5 receptors and the Schiff base ligand (**HL**) is possible. 2D plot curves of docking with Schiff base ligand (**HL**) are shown in Fig. 7. This interaction could activate apoptosis in cancer cells energy of interactions with Schiff base ligand (**HL**). Binding energies are most widely used as a mode of measuring binding affinity of a ligand. Thus, decrease in binding energy due to mutation will increase the binding affinity of the azo dye ligand towards the receptor. The characteristic feature of Schiff base ligand was represented in the presence of several active sites available for hydrogen bonding. This feature gives them the ability to be good binding inhibitors to the protein and will help to produce augmented inhibitory compounds.

Table 2
The calculated quantum chemical parameters for Schiff base ligand (**HL**).

E_{HOMO} (eV)	E_{LUMO} (eV)	ΔE (eV)	χ (eV)	η (eV)	σ $(eV)^{-1}$	Pi (eV)	S $(eV)^{-1}$	ω (eV)	ΔN_{max}
−6.569	−3.34	3.23	4.955	1.6145	0.6194	−4.955	0.3097	7.6021	3.0688

Table 3
Energy values obtained in docking calculations of Schiff base ligand (**HL**) with receptor prostate cancer mutant 2q7k and breast cancer mutant 3hb5.

Receptor	Free energy of binding (kCal/mol)	Inhibition constant (k_i) (μM)	vdW + bond + desolve energy (kCal/mol)	Electrostatic energy (kCal/mol)	Total intercooled energy (kCal/mol)	Interact surface
2q7k	−2.3	20.75	−3.75	+0.04	−3.71	631.524
3hb5	−7.3	4.43	−8.85	−0.06	−8.91	960.186

The results confirmed also that, the Schiff base ligand derived from 4-aminoantipyrine is an efficient inhibitor of prostate cancer mutant 2q7k-hormone and 3hb5-oxidoreductase breast cancer.

3.4. Potentiometric studies

The interaction of a metal with an electron donor atom of a Schiff base ligand (**HL**) is usually followed by the release of H^+. Alkaline potentiometric titrations are based on the detection of the protons released upon complexation. The main advantage of this technique, compared to other methods is that from the titration curves it is possible to follow complexation continuously as a function of pH and to detect exactly at which pH complexation takes place. Furthermore, it is possible to calculate the dissociation constant and the stability constants from the potentiometric titration curves. The average number of the protons associated with ligand (**HL**) at different pH values, $\overline{n}_{A,}$ was calculated from the titration curves of the acid in the absence and presence of ligand (**HL**) by applying the following equation:

$$\overline{n}_A = Y \pm \frac{(V_1 - V_2)(N^o + E^o)}{(V^o - V_1)TC_L^o} \tag{9}$$

where Y is the number of available protons in ligand (**HL**) (Y = 1) and V_1 and V_2 are the volumes of alkali required to reach the same pH on the titration curve of hydrochloric acid and reagent, respectively, $V°$ is the initial volume (50 cm^3) of the mixture, $TC°_L$ is the total concentration of the reagent, $N°$ is the normality of sodium hydroxide solution and $E°$ is the initial concentration of the free acid. Thus, the formation curves ($\overline{n}_A$ *vs.* pH) for the proton–ligand systems were constructed and found to extend between 0 and 1 in the $\overline{n}_A$ scale. This means that 4-aminoantipyrine Schiff base has one ionizable proton (the enolized hydrogen ion of the phenolic –OH group, pK^H). Different computational methods were applied to evaluate the dissociation constant [45]. Three replicate titrations were performed; the average values obtained are listed in Table 4. The completely protonated form of ligand (**HL**) has one dissociable proton, that dissociates in the measurable pH range. The deprotonation of the *o*-hydroxy group in the Schiff base ligand most probably results in the formation of stable intramolecular H-bonding with the nitrogen atom of the C═N group. Such an interaction decreases the dissociation process of 4-aminoantipyrine Schiff base, *i.e.* increases the pK^H value [46,47].

The formation curves for the metal complexes were obtained by plotting the average number of ligands attached per metal ion (n_A) *vs.* the free ligand exponent (pL), according to Irving and Rossotti [48]. The average number of the reagent molecules attached per metal ion, $\overline{n}$, and free ligand exponent, pL, can be calculated using Eqs. (10) and (11):

$$\overline{n} = \frac{(V_3 - V_2)(N^o + E^o)}{(V^o - V_2).\overline{n}_A.TC_M^o} \tag{10}$$

and

$$pL = \log_{10} \frac{\sum_{n=o}^{n=J} \beta_n^H \left(\frac{1}{[H^+]}\right)^n}{TC_L^o - \overline{n}.TC_M^o} \cdot \frac{V^o + V_3}{V^o} \tag{11}$$

where $TC°_M$ is the total concentration of the metal ion present in the solution, $\beta^H{}_n$ is the overall proton-reagent stability constant. V_1, V_2 and V_3

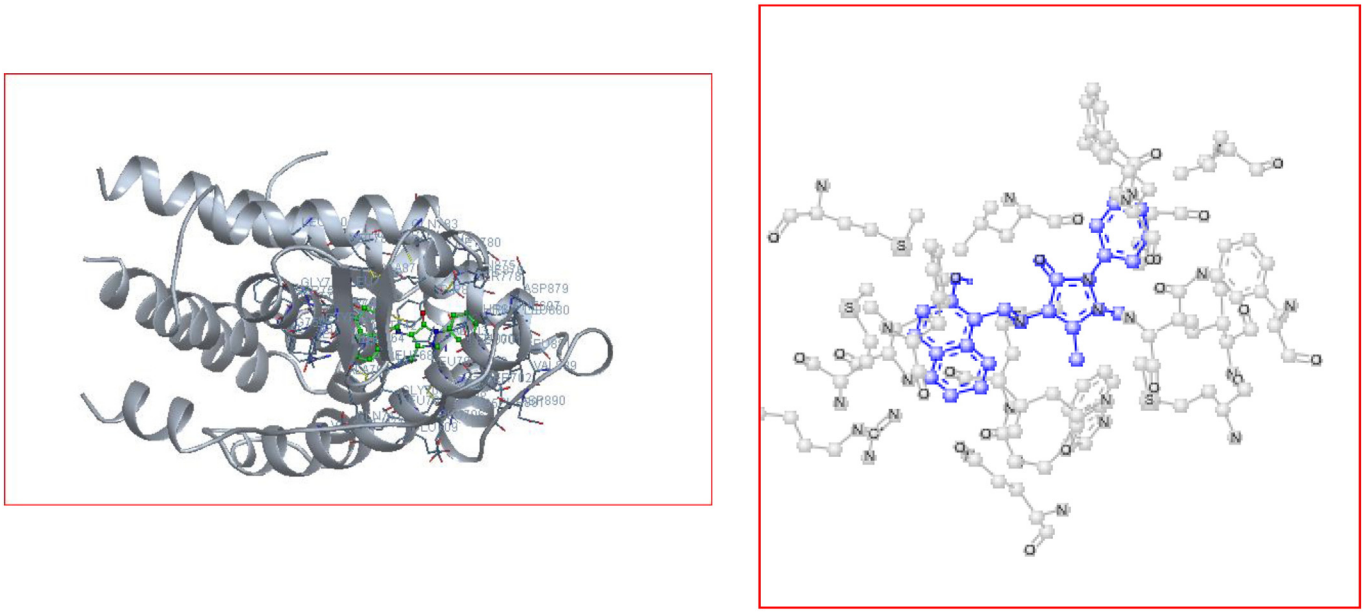

(A) (B)

Fig. 4. The Schiff base ligand (**HL**) (green in (A) and blue in (B)) in interaction with receptor prostate cancer mutant 2q7k. (For interpretation of the references to color in this figure legend, the reader is referred to the web version of this article).

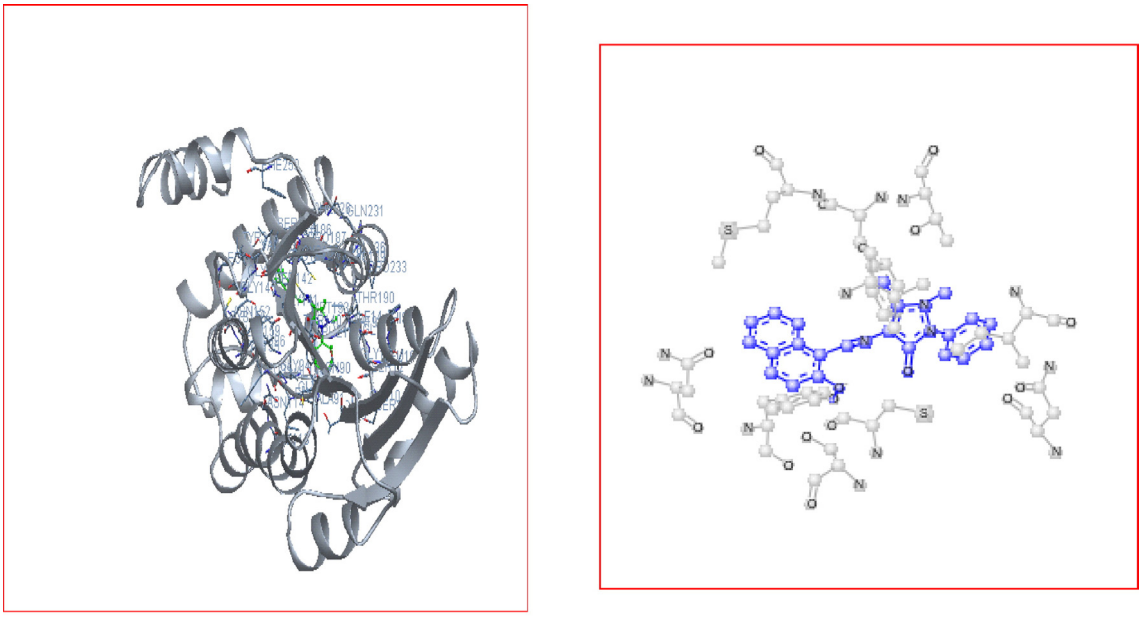

Fig. 5. The Schiff base ligand (**HL**) (green in (A1) and blue in (B1)) in interaction with receptor breast cancer mutant 3hb5. (For interpretation of the references to color in this figure legend, the reader is referred to the web version of this article.)

are the volumes of alkali required to reach the same pH on the titration curves of hydrochloric acid, organic ligand and complex, respectively. These curves were analyzed and the successive metal–ligand stability constants were determined using different computational methods [49,50]. The values of the stability constants (log K_1 and log K_2) are given in Table 5. The following general remarks can be pointed out:

(i) The maximum value of $\overline{n}$ was ~2 indicating the formation of 1:1 and 1:2 (metal:ligand) complexes only [1,51].

(ii) The metal ion solution used in the present study was very dilute (2×10^{-5} M), hence there was no possibility of formation of poly nuclear complexes [52,53].

(iii) The metal titration curves were displaced to the right-hand side of the ligand titration curves along the volume axis, indicating proton release upon complex formation of the metal ion. The large decrease in pH for the metal titration curves relative to ligand titration curves points to the formation of strong metal complexes [54,55].

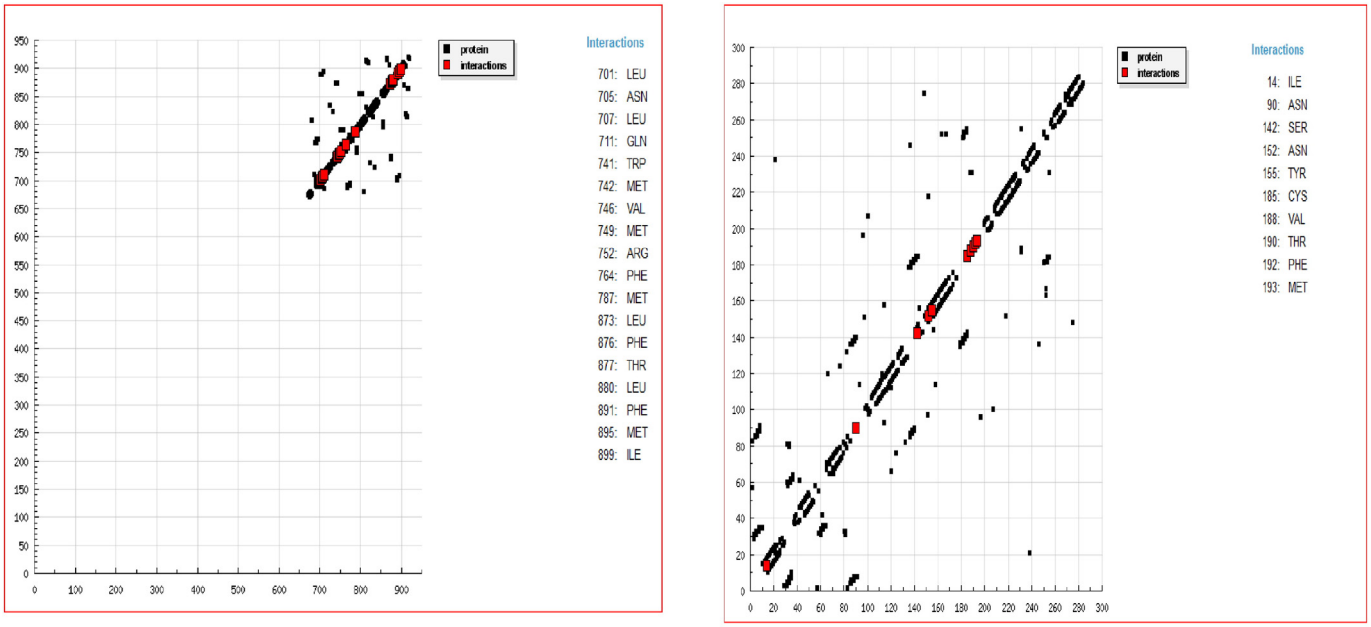

Fig. 6. HB plot of interaction between Schiff base ligand (**HL**) with receptor: a) prostate cancer mutant 2q7k and b) breast cancer mutant 3hb5.

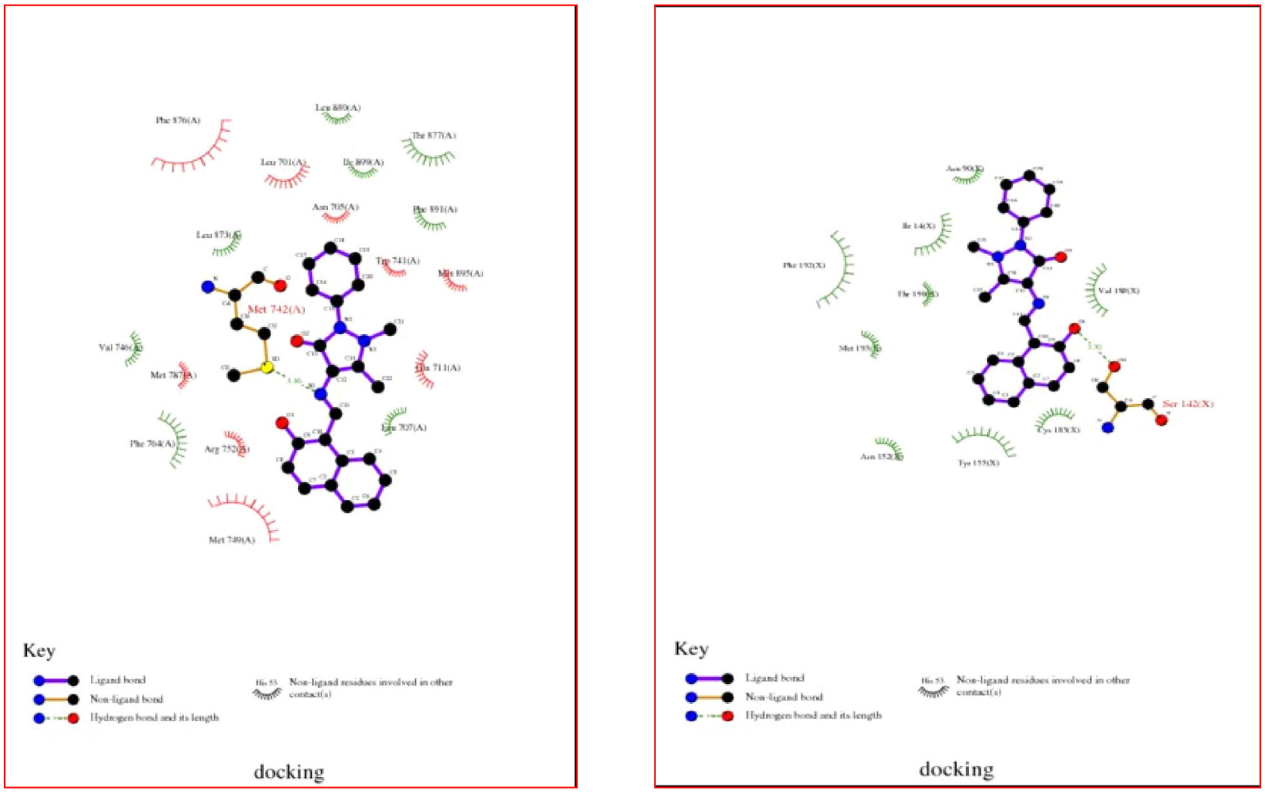

Fig. 7. 2D plot of interaction between Schiff base ligand (**HL**) with receptor: a) prostate cancer mutant 2q7k and b) breast cancer mutant 3hb5.

(iv) At constant temperature, the stability of the chelates increases in the order of $Cu^{2+} > Ni^{2+} > Co^{2+} > Mn^{2+}$ [56–58]. This order largely reflects that the stability of Cu^{2+} complexes is considerably larger than those of other metals of the 3d series. Under the influence of both the polarizing ability of the metal ion and the ligand field [59] Cu^{2+} will receive some extra stabilization due to tetragonal distortion of octahedral symmetry in its complexes. The greater stability of Cu^{2+} complexes is produced by the well known Jahn–Teller effect [60].

Stepwise dissociation constants for the ligand (**HL**) and the stepwise stability constants of their complexes with Mn^{2+}, Co^{2+}, Ni^{2+} and Cu^{2+} have been calculated at 298, 308 and 318 K. The corresponding thermodynamic parameters (ΔG, ΔH and ΔS) were evaluated.

The dissociation constants (pK^H) for **HL**, as well as the stability constants of its complexes with Mn^{2+}, Co^{2+}, Ni^{2+} and Cu^{2+} have been evaluated at 298, 308, 318 K and are given in Tables 4 and 5, respectively. The enthalpy (ΔH) for the dissociation and complexation process was calculated from the slope of the plot pK^H or log K *vs.* 1/T using the graphical representation of Van't Hoff (Eqs. (12) and (13)):

$$\Delta G = -2.303RT\log K = \Delta H - T\Delta S \tag{12}$$

or

$$\log K = \left(\frac{-\Delta H}{2.303R}\right)\left(\frac{1}{T}\right) + \frac{\Delta S}{2.303R} \tag{13}$$

where R gas constant = 8.314 J · mol^{-1} · K^{-1}, K is the dissociation constant for the ligand stability and T is the temperature (K).

From the ΔG and ΔH values, one can deduce the entropy ΔS using the well known relationships Eq. (12) and Eq. (14):

$$\Delta S = (\Delta H - \Delta G)/T. \tag{14}$$

The thermodynamic parameters of the dissociation process of **HL** are recorded in Table 4. From these results the following can be made:

(i) The pK^H values decrease with increasing temperature, *i.e.* the acidity of ligand increases [1].

Table 4
Thermodynamic functions for the dissociation of Schiff base ligand (**HL**) in 20% (by volume) DMF–water mixture in the presence of 0.1 M KCl at different temperatures.

Temperature (K)	Dissociation constant pK^H	Free energy charge (kJ mol^{-1}) ΔG	Enthalpy change (kJ mol^{-1}) ΔH	Entropy change (J mol^{-1} K^{-1}) −ΔS
298	9.32	53.18	33.57	65.82
308	9.13	53.84	33.57	65.83
318	8.95	54.49	33.57	65.82

Table 5
Stepwise stability constants for ML and ML_2 complexes of **HL** in 20% (by volume) DMF–water mixture in the presence of 0.1 M KCl at different temperatures.

M^{n+}	298 K		308 K		318 K	
	$\log K_1$	$\log K_2$	$\log K_1$	$\log K_2$	$\log K_1$	$\log K_2$
Mn^{2+}	5.08	4.15	5.17	4.24	5.28	4.35
Co^{2+}	5.25	4.32	5.35	4.42	5.45	4.53
Ni^{2+}	5.33	4.41	5.44	4.50	5.54	4.59
Cu^{2+}	5.45	4.54	5.56	4.65	5.67	4.75

(ii) Positive values of ΔH indicate that dissociation is accompanied by absorption of heat and the process is endothermic.
(iii) Large positive values of ΔG indicate that the dissociation process is not spontaneous [61].
(iv) Negative values of ΔS are due to increased order as a result of the solvation processes.

All the thermodynamic parameters of stepwise stability constants for the complexes of Schiff base ligand (**HL**) are recorded in Table 6. It is known that the divalent metal ions exist in solution as octahedral hydrated species [33] and the obtained values ΔH and ΔS can then be considered as a sum of two contributions: (a) Release of H_2O molecules and (b) metal–ligand bond formation. Examination of these values shows that:

(i) The stability constants (log K_1 and log K_2) for the 4-aminoantipyrine Schiff base complexes increase with increasing temperature, *i.e.* its stability constants increase with increasing temperature [1].
(ii) The stability constants of Mn^{2+}, Co^{2+}, Ni^{2+} and Cu^{2+} complexes were increased with increasing atomic number in the order of $Cu^{2+} > Ni^{2+} > Co^{2+} > Mn^{2+}$ at constant temperature.
(iii) The negative values of ΔG for the complexes formation suggest a spontaneous nature of such process [62].
(iv) The positive values of ΔH mean that the complex formation processes are endothermic and favored at higher temperature.
(v) The positive values of ΔS confirming that the complex formation processes are entropically favorable [62].

4. Conclusion

Schiff base ligand (**HL**) has been synthesized and characterized. The molecular and electronic structure of the investigated ligand (**HL**) was studied. Molecular docking was used to predict the binding between Schiff base ligand with the receptor of prostate cancer 2q7k-hormone and 3hb5-oxidoreductase receptor of breast cancer. The proton–ligand dissociation constant of **HL** and metal–ligand stability constants of its complexes with metal ions (Mn^{2+}, Co^{2+}, Ni^{2+} and Cu^{2+}) at different temperatures were determined. The stability constants of the formed complexes are increases in the order of $Cu^{2+} > Ni^{2+} > Co^{2+} > Mn^{2+}$. The dissociation process is non-spontaneous, endothermic and entropically unfavorable. The formation of the metal complexes has been found to be spontaneous, endothermic and entropically favorable.

Table 6
Thermodynamic functions for ML and ML_2 complexes of **HL** in 20% (by volume) DMF–water mixture and 0.1 M KCl.

M^{n+}	T/K	Free energy change ($kJ \cdot mol^{-1}$)		Enthalpy change ($kJ \cdot mol^{-1}$)		Entropy change ($J \cdot mol^{-1} \cdot K^{-1}$)	
		$-\Delta G_1$	$-\Delta G_2$	ΔH_1	ΔH_2	ΔS_1	ΔS_2
Mn^{2+}	298	23.28	29.44	24.48	21.81	160.26	171.97
	308	24.83	31.26			160.08	172.28
	318	26.49	32.88			160.26	171.96
Co^{2+}	298	24.19	30.24	20.85	23.58	151.15	180.61
	308	25.65	32.02			150.98	180.53
	318	27.22	33.85			151.15	180.61
Ni^{2+}	298	25.05	31.10	21.77	21.79	157.10	177.46
	308	26.60	32.91			157.02	177.57
	318	28.19	34.65			157.10	177.45
Cu^{2+}	298	25.90	32.01	21.77	21.77	159.97	183.40
	308	27.48	33.73			159.89	183.04
	318	29.10	35.68			159.97	183.41

References

[1] A.A. El-Bindary, A.Z. El-Sonbati, M.A. Diab, E.E. El-Katori, H.A. Seyam, Int. J. Adv. Res. 2 (2014) 493–502.
[2] M. Hong, H. Yin, X. Zhang, C. Li, C. Yue, S. Cheng, J. Organomet. Chem. 724 (2013) 23–31.
[3] H.K. Sharma, P. Dogra, A.K. Gupta, F. Koohyar, Quimera 37 (2014) 1324–1328.
[4] A. Başoğlu, S. Parlayan, M. Ocak, H. Alp, H. Kantekin, M. Ozdemir, U. Ocak, Polyhedron 28 (2009) 1115–1120.
[5] E. Hadjoidis, A. Rontoyianni, K. Ambroziac, T. Dziembowska, I.M. Marvidis, J. Photochem. Photobiol. A Chem. 162 (2004) 521–530.
[6] A. Oshima, A. Momotake, T. Arai, J. Photochem. Photobiol. A Chem. 162 (2004) 473–479.
[7] H. Josi, F.S. Kamounah, C. Gooijer, G. Zwan, L. Antonov, J. Photochem. Photobiol. A Chem. 152 (2002) 183–191.
[8] P. Fita, E. Luzina, T. Dziembowska, D. Kopec, P. Piatkowski, C. Radzewicz, a. Grabowska, Chem. Phys. Lett. 416 (2005) 305–310.
[9] S. Mahanta, R.B. Singh, S. Kar, N. Guchait, Chem. Phys. 324 (2006) 742–752.
[10] A.M. Asiri, K.O. Badahdah, S.A. Khan, A.G. Al-Sehemi, M.S. Al-Amoudi, A.A. Bukhari, Org. Chem. Insights 3 (2010) 1–8.
[11] A. Blagus, D. Cinčić, T. Friščić, B. Kaitner, V.S. Macedonian, J. Chem. Eng. 29 (2010) 117–138.
[12] H. Unver, M. Kabak, D.M. Zengin, T.N. Durlu, J. Chem. Crystallogr. 31 (2001) 203–209.
[13] M. Yıldız, H. Unver, D. Erdener, N. Ocak, A. Erdonmez, T.N. Durlu, Cryst. Res. Technol. 41 (2006) 600–606.
[14] Z. Rozwadowski, W. Schlif, B. Kamienski, Magn. Reson. Chem. 43 (2005) 573–577.
[15] J. Matijevic-Sosa, M. Vinkovic, D. Vikic-Topic, Croat. Chem. Acta 79 (2006) 489–495.
[16] S.H. Alarcon, A.C. Olivieri, D. Sanz, R.M. Claramunt, J. Elguero, J. Mol. Struct. 705 (2004) 1–9.
[17] P.V. Rao, C.P. Rao, E.K. Wegelius, K. Rissanen, J. Chem. Crystallogr. 33 (2003) 139–147.
[18] W.M.F. Fabian, L. Antonov, D. Nedeltcheva, F.S. Kamounah, P.J. Taylor, J. Phys. Chem. A 108 (2004) 7603–7612.
[19] L. Antonov, W.M.F. Fabian, D. Nedeltcheva, F.S. Kamounah, J. Chem. Soc., Perkin Trans. 2 (2000) 1173–1179.
[20] A.M. Asiri, K.O. Badahdah, Molecules 12 (2007) 1796–1804.
[21] W. Zeng, J. Li, Z. Mao, Z. Hong, S. Qin, Adv. Synth. Catal. 346 (2004) 1385–1391.
[22] A.A. El-Bindary, A.Z. El-Sonbati, M.A. Diab, A.M. Barakat, J. Appl. Sol. Chem. Model. 2 (2013) 191–196.
[23] A.T. Mubarak, A.S. Al-Shihri, H.M. Nassef, A.A. El-Bindary, J. Chem. Eng. Data 55 (2010) 5539–5542.
[24] A.T. Mubarak, A.A. El-Bindary, J. Chem. Eng. Data 55 (2010) 5543–5546.
[25] R.M. Issa, A.M. Khedr, H.F. Rizk, Spectrochim. Acta A 62 (2005) 621–629.
[26] N.A. El-Ghamaz, A.Z. El-Sonbati, M.A. Diab, A.A. El-Bindary, G.G. Mohamed, Sh.M. Morgan, Spectrochim. Acta A 147 (2015) 200–211.
[27] A.Z. El-Sonbati, M.A. Diab, A.A. El-Bindary, A.M. Eldesoky, Sh.M. Morgan, Spectrochim. Acta A 135 (2015) 774–791.
[28] A.F. Shoair, A.R. El-Shobaky, E.A. Azab, J. Mol. Liq. 203 (2015) 59–65.
[29] T.A. Halgren, J. Comput. Chem. 17 (1998) 490–519.
[30] G.M. Morris, D.S. Goodsell, J. Comput. Chem. 19 (1998) 1639–1662.
[31] R.G. Bates, M. Paabo, R.A. Robinson, J. Phys. Chem. 67 (1963) 1833–1838.
[32] H.M. Irving, M.G. Miles, L.D. Pettit, Anal. Chim. Acta 38 (1967) 475–488.
[33] G.H. Jeffery, J. Bassett, J. Mendham, R.C. Deney, Vogel's Textbook of Quantitative Chemical Analysis, 5th ed. Longman, London, 1989.
[34] S. Fazil, R. Ravindran, A.S. Devi, B.K. Bijili, J. Mol. Struct. 1021 (2012) 147–152.
[35] V. Mahalingam, N. Chitrapriya, F.R. Fronczek, K. Natarajan, Polyhedron 29 (2010) 3363–3371.
[36] F.A. Al-Saif, Int. J. Electrochem. Sci. 8 (2013) 10424–10445.
[37] B. Anupama, M. Padmaja, C.G. Kumari, E-J. Chem. 9 (1) (2012) 389–400.
[38] R. Prabhakaran, K. Palaniappan, R. Huang, M. Sieger, W. Kaim, P. Viswanathamurthi, F. Dallemer, K. Natarajan, Inorg. Chim. Acta 376 (2011) 317–324.
[39] M. Thomas, A. Kulandaisamy, A. Manohar, Chem. Tech. 4 (2012) 247–257.
[40] A.A. El-Bindary, A.Z. El-Sonbati, M.A. Diab, Sh.M. Morgan, J. Mol. Liq. 201 (2015) 36–42.
[41] N.A. El-Ghamaz, A.Z. El-Sonbati, M.A. Diab, A.A. El-Bindary, M.K. Awad, Sh.M. Morgan, Mater. Sci. Semicond. Process. 19 (2014) 150–162.
[42] A.Z. El-Sonbati, G.G. Mohamed, A.A. El-Bindary, W.M.I. Hassan, A.K. Elkholy, J. Mol. Liq. 209 (2015) 625–634.
[43] J.R. Benson, I. Jatoi, Future Oncol. 8 (2012) 697–702.
[44] A. Beteringhe, C. Racuciu, C. Balan, E. Stoican, L. Patron, Adv. Mater. Res. 787 (2013) 236–240.
[45] H. Irving, H.S. Rossotti, J. Chem. Soc. 76 (1954) 2904–2910.
[46] E. Farkas, H. Csoka, J. Inorg. Biochem. 89 (2002) 219–226.
[47] M.M. Omar, G.G. Mohamed, Spectrochim. Acta A 61 (2005) 929–936.
[48] H. Irving, H.S. Rossotti, J. Chem. Soc. 74 (1953) 3397–3405.
[49] F.J.C. Rossotti, H.S. Rossotti, Acta Chem. Scand. 9 (1955) 1166–1176.
[50] M.T. Beck, I. Nagybal, Chemistry of Complex Equilibrium, Wiley, New York, 1990.
[51] A.A. El-Bindary, A.Z. El-Sonbati, E.H. El-Mosalamy, R.M. Ahmed, Chem. Pap. 57 (2003) 255–258.
[52] P. Sanyal, G.P. Sengupta, J. Indian Chem. Soc. 67 (1990) 342–344.
[53] S. Sridhar, P. Kulanthaip, P. Thillaiarasu, V. Thanikachalam, G.J. Manikandan, World J. Chem. 4 (2009) 133–140.
[54] V.D. Athawale, V.J. Lele, Chem. Eng. Data 41 (1996) 1015–1019.
[55] V.D. Athawale, S.S. Nerkar, Monatsh. Chem. 131 (2000) 267–276.
[56] G.A. Ibañez, G.M. Escandar, Polyhedron 17 (1998) 4433–4441.

[57] W.U. Malik, G.D. Tuli, R.D. Madan, Selected Topics in Inorganic Chemistry, 3rd Ed. Chand S.& Company LTD, New Delhi, 1984.
[58] G.G. Mohamed, M.M. Omar, A. Ibrahim, Eur. J. Med. Chem. 44 (2009) 4801–4812.
[59] F.R. Harlly, R.M. Burgess, R.M. Alcock, Solution Equilibria, Ellis Harwood, Chichester, 1980 257.
[60] L.E. Orgel, An Introduction to Transition Metal Chemistry Ligand Field Theory, 1966 55 (Methuen, London).
[61] A. Bebot-Bringaud, C. Dange, N. Fauconnier, C. Gerard, J. Inorg. Biochem. 75 (1999) 71–78.
[62] A.Z. El-Sonbati, A.A. El-Bindary, R.M. Ahmed, J. Solut. Chem. 32 (2003) 617–623.